MATEC Web of Conferences **1**, 04005 (2012)
DOI: 10.1051/matecconf/20120104005
© Owned by the authors, published by EDP Sciences, 2012

Theoretical and experimental investigation of the nonlinear response of an electrically actuated imperfect microbeam

L. Ruzziconi[1], A. M. Bataineh[2], M. I. Younis[2], and S. Lenci[1]

[1] Department of Civil and Building Engineering, and Architecture, Polytechnic University of Marche, 60131 Ancona, Italy
[2] Department of Mechanical Engineering, State University of New York at Binghamton, Binghamton, 13902 NY, USA
E-mails: l.ruzziconi@univpm.it; abatain1@binghamton.edu; myounis@binghamton.edu; lenci@univpm.it

Abstract. In this study a theoretical and experimental investigation of the nonlinear response of an electrically actuated microbeam is performed. A mechanical model is proposed, which accounts for two common imperfections of microbeams, due to microfabrications, which are the compliant support conditions and the initially deformed profile. A computationally efficient single-mode reduced-order model is derived by combining the Ritz technique and the Padé approximation. Numerical simulations of the harmonic response of the device near primary resonance are shown illustrating nonlinear phenomena arising in the device response. Experimental investigation is conducted on a polysilicon imperfect microbeam confirming the simulation results. The concurrence between the theoretical results and the experimental data reveals that this model, while simple, is capable of properly capturing the response both at low and, especially, at higher electrodynamic voltages.

1 Introduction

Microelectromechanical systems (MEMS) are largely used in a wide spectrum of applications and in a variety of different fields, where they have many different functions, including sensing, actuation, and signal processing [1, 2].

Simulating their complex dynamics accurately and properly requires careful modelling. Numerous studies emphasise the importance of generating reduced-order models, which are able to produce reliable results without excessive computational effort. Many approaches based on the Galerkin technique have been proposed in the literature. They mainly focus on the electric term, which is difficult to be analyzed directly and has been addressed using many different procedures. Younis *et al.* [3] developed a Galerkin reduced-order model based on multiplying the equation of motion with the denominator of the electrostatic force term. This approach requires only few modes to converge. It was adopted in several case-studies, such as electrically actuated microbeams and arches, with good agreement reported between theoretical results and experimental data for both the static and dynamic problems [3, 4]. Krylov and Dick [5] adopted a suitable shape function, which was able to considerably simplify the expression for the electric contribution. Ouakad and Younis [6], investigating carbon nanotube resonators, developed a reduced-order model, which relies on numerical integration of the electrostatic force term at every time step, which was proven to yield fairly accurate results, although time-consuming. Rhoads *et al.* [7], before applying the Galerkin method, approximated the electric term through a truncated Taylor expansion. This leads to a rather simple reduced-order model, which is accurate for a "small" displacement. Ruzziconi *et al.* [8] proposed a simple and efficient reduced-order model based on combining the Galerkin technique and the Padé approximation. It is able to analyze the device response not only at low electrodynamic voltages, but also at large values, where the inevitable escape (dynamic pull-in) becomes impending.

This paper deals with the MEMS device of figure 1, which is an electrically actuated imperfect microbeam. The actual dimensions are experimentally measured and an experimental parametric study of its response in a neighbourhood of the natural frequency is performed. A mechanical model is presented, which takes into account both the initial deformed configuration of microbeam and the flexible supports. A reduced-order model is introduced, according to the procedure proposed in [8]. We show a satisfactory concurrence between theoretical and experimental results, which is achieved both at low and, remarkably, at higher electrodynamic excitation.

The paper is organized as follows. The MEMS device is experimentally tested (Sec. 2), the mechanical model is introduced (Sec. 3), a single d.o.f. reduced-order model is derived (Sec. 4), nonlinear dynamic simulations are

This is an Open Access article distributed under the terms of the Creative Commons Attribution License 2.0, which permits unrestricted use, distribution, and reproduction in any medium, provided the original work is properly cited.

performed, which validate the model (Sec. 5), and the main conclusions are summarized (Sec. 6).

2 Experimental data

Figure 1 shows a top-view of the experimentally tested MEMS device, which consists of a polysilicon microbeam actuated by an electrode placed directly underneath it on a substrate. The figure also illustrates the actuation pads on both sides of the microbeam, which are used to actuate the device electrically. Typically, these pads have some flexibility, due to under-etching from fabrications, which needs to be accounted for in the model.

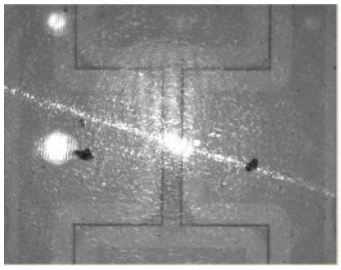

Fig. 1. A picture of the tested MEMS device showing the laser dot of the laser Doppler vibrometer.

Since the model results are sensitive to the geometry, the actual dimensions of the device are measured directly. For this, a Wyko profilometer is used to map the topography of the device, as shown in figure 2, which visualizes the measured profile at rest and without any electric load. The measured length is $l = 392.82$ µm, the width is $b = 43.7$ µm, and the maximum initial rise is 5.3 µm.

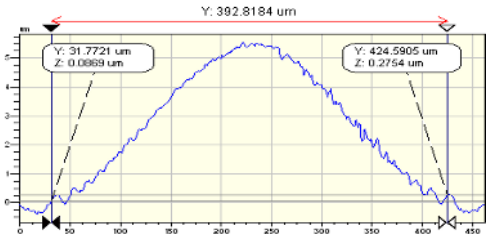

Fig. 2. Actual microbeam profile in microns at rest.

We present data of dynamic testing conducted using a high-frequency laser Doppler Vibrometer (MSA-MEMS motion analyzer) under reduced pressure (low damping conditions). Using a random signal excitation, the linear fundamental resonance frequency is found to be $\Omega \cong$ 145.86 kHz (figure 3).

The other parameters values are derived in order to have a good agreement between the theoretical results and the experimental frequency response. In particular, we consider the microbeam thickness equal to $h = 1.1$ µm and the initial rise as constituted by 3.6 µm of arched configuration and 1.7 µm of deflection due to residual stresses. For the gap, we use $d = 1$ µm.

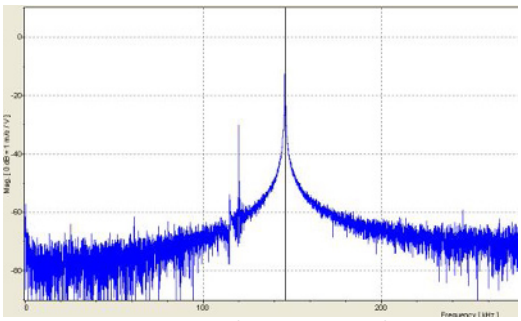

Fig. 3. Measured first resonance frequency.

Experimental frequency sweep tests are conducted at a DC voltage load of $V_{DC} = 0.7\,V$, which yield frequency response curves of the maximum amplitude of the oscillations. In the frequency-sweeping process, the dynamic voltage (AC load amplitude V_{AC}) is kept constant and the frequency is increased (forward sweep) or decreased (backward sweep) slowly, i.e. quasi-statically. The frequency step is 5 Hz and the pressure is 60-70 mtorr. Examples are reported in figure 4.

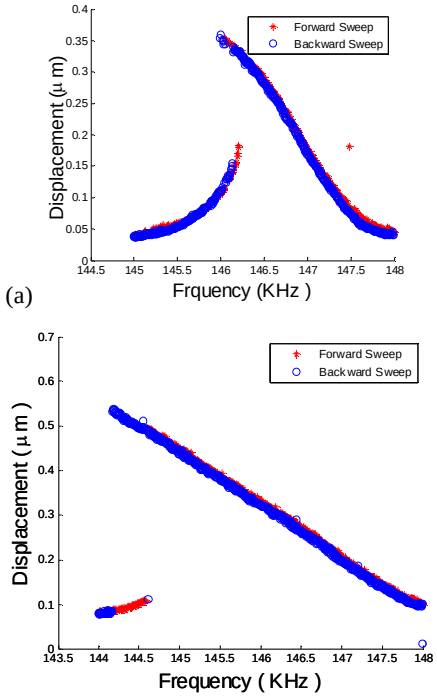

Fig. 4. Experimental frequency response curves at (a) $V_{AC} = 1.5\,V$; (b) $V_{AC} = 2.6\,V$. The forward and backward sweep are respectively in red and blue.

3 Mechanical model

A schematic of the tested MEMS device is illustrated in figure 5. To simulate non-ideally fixed-fixed boundary conditions, translational and rotational springs have been added at each edge. The shallow arched initial shape is delineated by $y_0(z) = \frac{1}{2} y_0(1 - \cos(2\pi z))$, where y_0 is the maximum initial rise. The electrode generates both an electrostatic and an electrodynamic excitation. Only the viscous damping contribution is considered, since is generally the most relevant source of energy loss in typical MEMS [2].

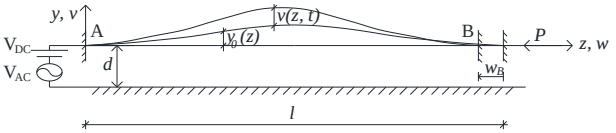

Fig. 5. A schematic of the MEMS device.

The microbeam is described in the framework of the Euler-Bernoulli theory and a linearly elastic isotropic and homogeneous material is supposed. We assume the shallow arched approximation. The nondimensional potential energy is

$$V = \frac{1}{2}\int_0^1 (v''(z,t))^2 dz + \frac{ka}{2}\int_0^1 \left(\beta w'(z,t) + \frac{1}{2}(v'(z,t))^2 + v'(z,t)y'_0(z)\right)^2 dz - \gamma V_{DC}^2 \int_0^1 \frac{1}{1+v(z,t)+y_0(z)} dz + \frac{1}{2}k\, v(0,t)^2 + \frac{1}{2}k\, v(1,t)^2 + \frac{1}{2}k_r\, v'(0,t)^2 + \frac{1}{2}k_r\, v'(1,t)^2 \quad (1)$$

which consists of the stain energy of the microbeam, the potential of the external electrostatic force and the potential of the springs. The axial displacement $w(z,t)$ is "condensed" by a classical procedure [9]. Applying Lagrange's method and adding damping and force, the resulting nondimensional equation of motion becomes

$$\ddot{v}(z,t) + \xi\, \dot{v}(z,t) + v''''(z,t) + \alpha\left(v''(z,t) + y''_0(z)\right) = -\gamma \frac{(V_{DC} + V_{AC}\cos(\Omega t))^2}{(1 + v(z,t) + y_0(z))^2} \quad (2)$$

where

$$\alpha = -ka\left(\int_0^1 \left(\frac{1}{2}(v'(z,t))^2 + v'(z,t)y'_0(z)\right) dz\right) \quad (3)$$

and the boundary conditions are

$$\begin{aligned} &\alpha\, v'(0,t) + v'''(0,t) + k\, v(0,t) = 0,\\ &v''(0,t) - k_r\, v'(0,t) = 0,\\ &\alpha\, v'(1,t) + v'''(1,t) - k\, v(1,t) = 0,\\ &v''(1,t) + k_r\, v'(1,t) = 0. \end{aligned} \quad (4)$$

The superimposed dot and prime in the formulas (1)-(4) denote the derivative with respect to the nondimensional time t and space z, respectively. The nondimensional variables used in (1)-(4) are (denoted by hats, which are dropped in (1)-(4) for convenience)

$$\tilde{z} = \frac{z}{l} \qquad \tilde{v} = \frac{v}{d} \qquad \tilde{y}_0 = \frac{y_0}{d} \qquad \tilde{w} = \frac{w}{d} \qquad \tilde{t} = \frac{t}{T} \quad (5)$$

and the nondimensional parameters are

$$\begin{aligned} &ka = (EA)d^2/(EJ) && \tilde{\Omega} = \Omega\, T\\ &\gamma = \frac{1}{2}\varepsilon_0\varepsilon_r A_c l^3/(d^3 EJ) && \tilde{k} = k\, l^3/(EJ)\\ &T = \sqrt{(\rho A\, l^4)/(EJ)} && \tilde{k}_r = k_r\, l\,/(EJ)\\ &\xi = c\, l^4/(EJ\, T) && \beta = l/d \end{aligned} \quad (6)$$

where ρA is the mass density per unit length, EA is the axial stiffness, EJ is the bending stiffness, A and J are the area and the moment of inertia of the cross section, E is the effective Young's modulus, ρ is the material density, d is the gap width between the stationary electrode and the undeformed straight position of the microbeam, $A_c = bl$ is the overlapped area between the microbeam and the stationary electrode, ε_0 is the dielectric constant in the free space, ε_r is the relative permittivity of the gap space medium with respect to the free space, c is the viscous damping coefficient, k and k_r are respectively the translational and rotational stiffness.

Referring to the microbeam experimentally tested in Sec. 2, the parameters of Eq. (2) are calculated as: $ka = 9.73947$, $T = 0.0000592566$, $\xi = 0.08$, $\gamma = 6.00525$. The nondimensional stiffness coefficients are estimated as $k = 12600$ and $k_r = 9.45$, which are based on the obtained natural frequency of the microbeam.

4 Reduced-order model

After analyzing the static and the linearized unforced undamped dynamics, we use these results to generate a reduced-order model [10].

The microbeam deflection $v(z,t)$ is approximated by $v(z,t) \cong v_s(z) + \sum_{i=1}^{M} \phi_i(z) Y_i(t)$. We consider the single (first symmetric) mode reduced-order model ($M = 1$), and we select the shape functions $v_s(z)$ and $\phi(z)$, respectively, equal to the stable static configuration and to the aforementioned mode shape. We apply the Ritz method to the potential form (1). The total potential energy function becomes

$$V(Y) = 1497.4\, Y^2 - 1042.34\, Y^3 + 379.744\, Y^4 - 2.94257 \int_0^1 \frac{\mathrm{d}z}{(1 + y_0(z) + v_s(z) + Y\phi(z))} \quad (7)$$

where $Y(t)$ is the amplitude of the displacement of the mode shape. In (7) we can directly compute the coefficients in the part due to the geometrical nonlinearity, while this is not possible for the part due to the electric force term, because the integral cannot be solved analytically. Since this expression for the electric potential is too complicated and time-consuming for nonlinear dynamic simulations, we attain an approximation of this term by the Padé expansion. To determine the Padé coefficients we require conditions, which retain the significant quantitative and qualitative aspects of the dynamics, such as the presence of a maximum in $V(Y)$, after which there is the transition to the escape. This yields to the total potential energy

$$V(Y) = 1497.4\, Y^2 - 1042.34\, Y^3 + 379.744\, Y^4 - \frac{2.40219}{2.51323 - Y} \quad (8)$$

A plot of Eq. (8) is depicted in figure 6. The single d.o.f. reduced-order model becomes

$$\ddot{Y} + 0.15\, \dot{Y} + 2994.81\, Y - 3127.01\, Y^2 + 1518.98\, Y^3 - \frac{4.90242}{(2.51323 - Y)^2}(0.7 + V_{AC}\cos(\Omega t))^2 = 0 \quad (9)$$

which is examined in the forthcoming analysis.

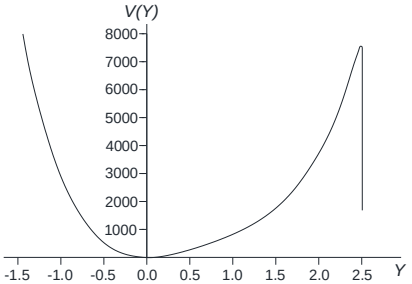

Fig. 6. The potential energy $V(Y)$ as expressed in (8).

5 Numerical simulations

We calculate the frequency response curves for the same voltage values previously investigated in figure 4. These numerical results have been obtained by using self-developed codes, based on direct integration and Runge-Kutta method. The results are reported in dimensions to facilitate the comparison with the experimental data.

These results show a good matching between the theoretical and the experimental curves. In a neighborhood of the resonance, the device exhibits a softening behavior. The non-resonant and resonant branches have the characteristic bending toward lower frequencies. The experimental branches exist for a smaller range than the theoretical one, but along these interval, the curves nearly coincide. Both the gap between the two branches, the range where the two attractors coexist and the bending are adequately represented. This occurs not only at low electrodynamic voltages (figure 7a) but also at higher ones (figure 7b).

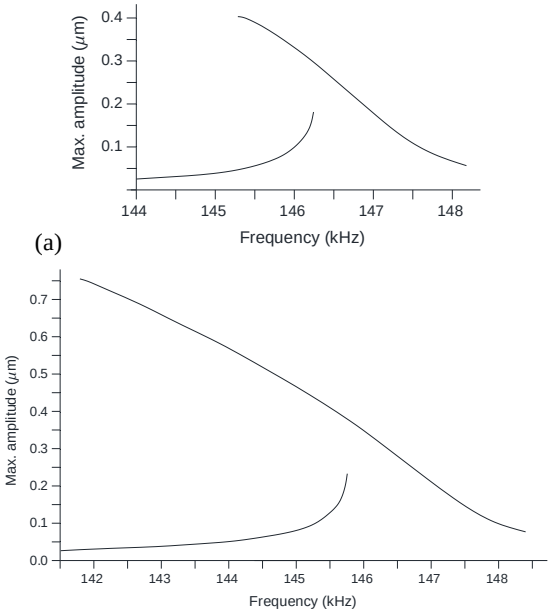

Fig. 7. Theoretical frequency response diagrams (in dimensional form) at (a) $V_{AC} = 1.5\,V$; (b) $V_{AC} = 2.6\,V$.

These results may be considered as an effective validation of the proposed reduced-order model. In fact, this reveals that, despite the apparent simplicity, the model is able to catch the most relevant nonlinear phenomena arising in the MEMS response and to represent them properly and accurately.

For sake of completeness, we note that the presence of a longer range of existence of both the branches in the theoretical simulations is due to dynamical integrity reasons, as observed in the case-study of a MEMS capacitive accelerometer [11].

6 Conclusions

A MEMS device based on an electrically actuated microbeam has been experimentally investigated. Frequency response curves have been obtained by a sweeping process in a neighborhood of the first symmetric natural frequency.

After introducing a mechanical model which takes into account imperfections both in the profile and in the boundary conditions, a single d.o.f. reduced-order model has been proposed. It is based on combining the Ritz technique and the Padé approximation. Despite the apparent simplicity of the model, the theoretical results show a satisfactory agreement with the experimental frequency response curves. The model is able to catch, properly and accurately, the most relevant aspects of the nonlinear MEMS response, both at low and, remarkably, at higher electrodynamic voltage excitations. This validates the proposed approach.

Acknowledgement

The authors would like to thank Dr. W. Cui for providing the fabricated MEMS device. This work has been supported in part by the National Science Foundation through grant # 0846775.

References

1. S. D. Senturia, *Microsystem Design* (Kluwer Academic Publishers, Dordrecht, 2001)
2. M. I. Younis, *MEMS Linear and Nonlinear Statics and Dynamics* (Springer, 2011)
3. M. I. Younis, E. M. Abdel-Rahman, A. H. Nayfeh, J. Microelectromech. Sys., **12**(5), 672-680 (2003).
4. H. M. Ouakad, M. I. Younis, Int. J. Non-Linear Mech., **45**, 704-713 (2010).
5. S. Krylov, N. Dick, Continuum Mech. Thermodyn., **22**, 445-468 (2010).
6. H. M. Ouakad, M. I. Younis, J. Comp. Nonlin. Dyn., **5**, 011009 (2010).
7. J. F. Rhoads, S. W. Shaw, K. L. Turner, J. Micromech. Microeng., **16**, 890–899 (2006).
8. L. Ruzziconi, M. I. Younis, S. Lenci, J. Comput. Nonlinear Dynamics (submitted for publication).
9. P. Villaggio, *Mathematical Models for Elastic Structures* (Cambridge University Press, Pisa, 1997).
10. G. Rega, H. Troger, Nonlinear Dyn., **41**, 1–15 (2005).
11. L. Ruzziconi, M. I. Younis, S. Lenci, IUTAM Symp. on Nonlinear Dynamics for Advanced Technologies and Engineering Design, Aberdeen (July 2010).